

MULTIPLE-INPUT MULTIPLE-OUTPUT LONGITUDINAL ROBUST CONTROL FOR AIRCRAFT

Nguyen Tien Hung

TNU - University of Technology

ARTICLE INFO	ABSTRACT
<p>Received: 19/6/2021</p> <p>Revised: 29/6/2021</p> <p>Published: 30/6/2021</p>	<p>This paper is dealt with the design of a multiple-input multiple-output robust controller for the longitudinal flight dynamics of an aircraft control system. The design objective is to achieve robust stability and good dynamic performance against the variation of aircraft parameters in which the aircraft forward speed is considered to be a real uncertainty. The controller synthesis is aimed at maintaining robust performance for frozen values of the aircraft forward speed in a specified operating range. The proposed robust controller is implemented using the robust control toolbox in Matlab. The obtained results verify the performance of the proposed controller for aircraft control system with respect to different values of the aircraft forward speeds.</p>
<p>KEYWORDS</p> <p>Flight control</p> <p>Robust controller</p> <p>Mixed sensitivity approach</p> <p>Loop-shaping design</p> <p>Robust performance</p>	

ĐIỀU KHIỂN BỀN VỮNG ĐA BIẾN CHUYỂN ĐỘNG DỌC CỦA CÁC THIẾT BỊ BAY

Nguyễn Tiến Hưng

Trường Đại học Kỹ thuật Công nghiệp – ĐH Thái Nguyên

THÔNG TIN BÀI BÁO	TÓM TẮT
<p>Ngày nhận bài: 19/6/2021</p> <p>Ngày hoàn thiện: 29/6/2021</p> <p>Ngày đăng: 30/6/2021</p>	<p>Bài báo này trình bày việc thiết kế bộ điều khiển bền vững đa biến cho mô hình động học chuyển động dọc của hệ thống điều khiển bay. Mục tiêu của bài toán thiết kế là nhằm đạt được tín ổn định bền vững với chất lượng động học mong muốn để chống lại các biến đổi tham số trong mô hình máy bay với vận tốc của máy bay được coi là một bất định. Việc tổng hợp bộ điều khiển là nhằm duy trì chất lượng động học bền vững của hệ thống khi vận tốc của máy bay nằm trong một khoảng xác định trước. Bộ điều khiển bền vững được thực hiện nhờ hộp công cụ Matlab. Các kết quả nghiên cứu đã kiểm chứng chất lượng của bộ điều khiển đối với các giá trị khác nhau của vận tốc máy bay.</p>
<p>TỪ KHÓA</p> <p>Điều khiển bay</p> <p>Bộ điều khiển bền vững</p> <p>Phương pháp độ nhạy hỗn hợp</p> <p>Thiết kế Loop-shaping</p> <p>Chất lượng bền vững</p>	

DOI: <https://doi.org/10.34238/tnu-jst.4672>

Email: h.nguyentien@tnut.edu.vn

<http://jst.tnu.edu.vn>

38

Email: jst@tnu.edu.vn

1. Introduction

In flight control systems, the performance requirements should be maintained over the entire range of aircraft speeds and altitudes. For improving the performance of the closed-loop longitudinal control, multi-input multi-output (MIMO) controller designs can be employed for both elevator and throttle servos with the linear quadratic regulator (LQR) control [1, 2]. On the other hand, it is well-known in flight control that the actuator dynamics depend on angle of attack regions [3]. In order to improve the system robustness against changes in the machine parameters and exogenous inputs, several controller designs have been proposed for such aircraft in literature. In [2, 4], the H_∞ controller design is proposed for multivariable vertical short take-off and landing (VSTOL) aircraft system. In [1], the same approach is also applied to generic VSTOL aircraft model. H_∞ control provides a very powerful tool for controller synthesis of multivariable linear time-invariant systems in the presence of uncertainty. However, the design techniques become more complicated if we consider uncertain linear time-varying systems. At the expense of conservativeness and possibly poor performance, the varying parameters can be treated as uncertainties and a single robust parameter-independent LTI controller can be designed for the entire operating range. On the other hand, if the parameter value is measurable online, one might instead try to design a parameter-dependent controller in order to improve performance. Recently, the linear parameter-varying (LPV) control approach, which takes the parameter variations into account directly in the control design, is applied for flight control systems of several types of aircraft and flight conditions [3, 5–7].

A common feature of the above publications is that the mathematical models of aircraft are not provided explicitly for some reasons. Furthermore, the robustness of the controlled system with respect to the changes of parameters is not also given clearly. Therefore, a robust H_∞ controller design to improve the performance of the elevator deflection control loop with respect to machine parameter variations and in view of the throttle servos disturbance is presented in [8]. The obtained results show that the designed H_∞ controller achieves the required performance specifications over the operating range of the aircraft. In addition, robustness of the controlled system against parameter changes as well as the impact of throttle servos on the robustness of the control system are also considered by means of some substantial simulation results. Since the throttle servo is considered to be a disturbance input, this design falls into the category of the single-input single-output (SISO) configuration. However, as it will be shown in the next section, the longitudinal dynamics model of aircraft is described by a MIMO system. Therefore, in order to improve the performance of the closed-loop control system, the effect of the crossing-term in the aircraft model should be taken into account. In this work, we present a MIMO robust H_∞ controller design that guarantees the tracking performance for both channels from the references to their corresponding outputs over the specified range of the aircraft forward speed. In addition, robustness of the controlled system against changes of aircraft parameter is also evaluated. The study results will be given to demonstrate the obtain performance of the proposed controller design.

In the next section, we will present the longitudinal dynamics model of aircraft. This model can be found in [8] but it is reproduced here for the reader's convenience. The multiple-objective H_∞ controller synthesis for a class of linear time-invariant systems

will be given as the content of the design section. Similarly to the previous work in [8], the method presented in this section is especially focused on affine parameter-dependent systems. The synthesis is based on the linear matrix inequality (LMI) approach and the bounded real lemma as a powerful tool for turning H_∞ -constraints into LMIs. More detail of the approach can be found in the literature, for instance in [9–11]. Finally, some simulation results and conclusions will be presented in the last sections.

2. Longitudinal dynamics model of aircraft

Consider the aircraft body axes, (i, j, k) and the north, east, down (NED) local horizon frame, (I, J, K) as shown in Figure 1. Note that longitudinal motion is normally represented by a small displacement from an equilibrium (unaccelerated) flight condition in the longitudinal plane. The flight variables in such an equilibrium are denoted with a subscript e . In this fashion, the pitch angle can be represented as $\Theta = \theta_e + \theta$. Similarly, the forward speed $U = U_e + u$, the downward (or plunge) velocity $W = v$, the pitch rate $Q = q$, the forward force $X = X_e + \bar{X}$, the downward force $Z = Z_e + \bar{Z}$, and the pitching moment $M = \bar{M}$ where $\theta, u, w, q, \bar{X}, \bar{Z}, \bar{M}$ are the perturbation quantities. Let $\mathbf{J} = (J_{ik})|_{i,k=\{x,y,z\}}$ be the inertia tensor, where J_{xx}, J_{yy}, J_{zz} are the moments of inertia, and J_{xy}, J_{yz}, J_{xz} are the products of inertia. Note that, for a symmetrical plane, $J_{xy} = J_{yz} = 0$. Let α be the angle of attack, m be the aircraft's mass, X be the forward force, Z be the downward force, M be the pitching moment, U be the forward speed. Denote $F_x = \frac{\partial F}{\partial x}|_e$, where $F \in \{X, Z, M\}$, as the first-order of a Taylor series expansion at the equilibrium point.

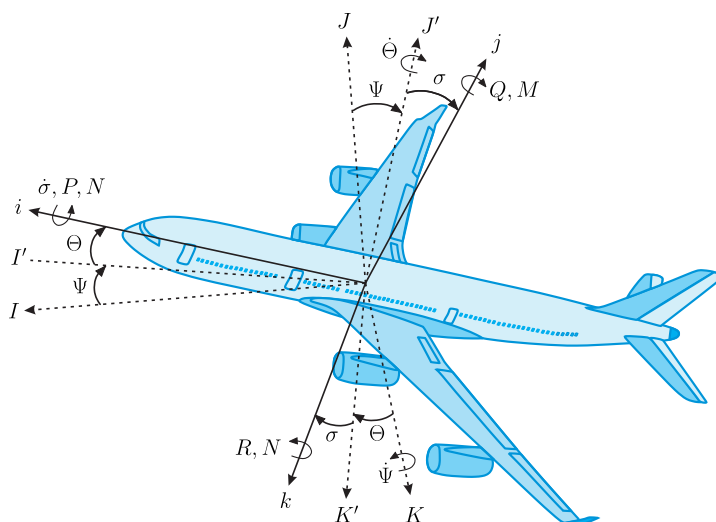


Figure 1. The aircraft body axes [1]

By neglecting products of small perturbation quantities, we obtain the longitudinal dynamics model of the aircraft in the state-space form as [1]

$$\dot{x}_l = A_l x_l + B_l w_l \tag{1}$$

$$y_l = C_l x_l \tag{2}$$

where

$$A_l = \begin{pmatrix} \frac{X_u}{m} & \frac{X_\alpha}{m} & -g \cos \theta_e & 0 \\ \frac{Z_u}{mU} & \frac{Z_\alpha}{mU} & -\frac{g \sin \theta_e}{U} & 1 + \frac{Z_q}{mU} \\ 0 & 0 & 0 & 1 \\ \frac{M_u}{J_{yy}} + \frac{M_{\dot{\alpha}} Z_u}{mU J_{yy}} & \frac{M_\alpha}{J_{yy}} + \frac{M_{\dot{\alpha}} Z_\alpha}{mU J_{yy}} & -\frac{M_{\dot{\alpha}} g \sin \theta_e}{U J_{yy}} & \frac{M_q}{J_{yy}} + \frac{M_{\dot{\alpha}}(mU + Z_q)}{mU J_{yy}} \end{pmatrix}, \quad (3)$$

$$B_l = \begin{pmatrix} \frac{X_\delta}{m} & \frac{X_T}{m} \\ \frac{Z_\delta}{mU} & \frac{Z_T}{mU} \\ 0 & 0 \\ \frac{M_\delta}{J_{yy}} + \frac{M_{\dot{\alpha}} Z_\delta}{mU J_{yy}} & \frac{M_T}{J_{yy}} + \frac{M_{\dot{\alpha}} Z_T}{mU J_{yy}} \end{pmatrix}, \quad C_l = \begin{pmatrix} 1 & 0 & 0 & 0 \\ 0 & 0 & 0 & 1 \end{pmatrix}, \quad (4)$$

$x_l = (u \ \alpha \ \theta \ q)^T$ is the state variable, $w_l = (\delta_E \ \beta_T)^T$ is the input of the system, δ_E is the elevator deflection, β_T is the throttle servos.

Let $v_a = \frac{1}{U}$ and express v_a as an uncertainty element $v_a = v_n(1 + p_v \delta_v)$, where v_n is the nominal value of v_a , $p_v \in \mathbb{R}$ indicates the variation of v_a around its nominal value, $\delta_v \in \mathbb{R}$, $-1 \leq \delta_v \leq 1$, we can write

$$A_l = A_{ln} + \delta_v A_{lv} \quad (5)$$

$$B_l = B_{ln} + \delta_v B_{lv} \quad (6)$$

in which

$$A_{ln} = \begin{pmatrix} \frac{X_u}{m} & \frac{X_\alpha}{m} & -g \cos \theta_e & 0 \\ \frac{Z_u}{m} v_n & \frac{Z_\alpha}{m} v_n & -g \sin \theta_e v_n & 1 + \frac{Z_q}{m} v_n \\ 0 & 0 & 0 & 1 \\ \frac{M_u}{J_{yy}} + \frac{M_{\dot{\alpha}} Z_u}{m J_{yy}} v_n & \frac{M_\alpha}{J_{yy}} + \frac{M_{\dot{\alpha}} Z_\alpha}{m J_{yy}} v_n & -\frac{M_{\dot{\alpha}} g \sin \theta_e}{J_{yy}} v_n & \frac{M_q}{J_{yy}} + \frac{M_{\dot{\alpha}}}{J_{yy}} + \frac{M_{\dot{\alpha}} Z_q}{m J_{yy}} v_n \end{pmatrix} \quad (7)$$

$$A_{lv} = \begin{pmatrix} 0 & 0 & 0 & 0 \\ \frac{Z_u}{m} v_n p_v & \frac{Z_\alpha}{m} v_n p_v & -g \sin \theta_e v_n p_v & \frac{Z_q}{m} v_n p_v \\ 0 & 0 & 0 & 0 \\ \frac{M_{\dot{\alpha}} Z_u}{m J_{yy}} v_n p_v & \frac{M_{\dot{\alpha}} Z_\alpha}{m J_{yy}} v_n p_v & -\frac{M_{\dot{\alpha}} m g \sin \theta_e}{m J_{yy}} v_n p_v & \frac{M_{\dot{\alpha}} Z_q}{m J_{yy}} v_n p_v \end{pmatrix} \quad (8)$$

$$B_{ln} = \begin{pmatrix} \frac{X_\delta}{m} & \frac{X_T}{m} \\ \frac{Z_\delta}{m} v_n & \frac{Z_T}{m} v_n \\ 0 & 0 \\ \frac{M_\delta}{J_{yy}} + \frac{M_{\dot{\alpha}} Z_\delta}{m J_{yy}} v_n & \frac{M_T}{J_{yy}} + \frac{M_{\dot{\alpha}} Z_T}{m J_{yy}} v_n \end{pmatrix} \quad B_{lv} = \begin{pmatrix} 0 & 0 \\ \frac{Z_\delta}{m} v_n p_v & \frac{Z_T}{m} v_n p_v \\ 0 & 0 \\ \frac{M_{\dot{\alpha}} Z_\delta}{m J_{yy}} v_n p_v & \frac{M_{\dot{\alpha}} Z_T}{m J_{yy}} v_n p_v \end{pmatrix} \quad (9)$$

Equation (1) can now be expressed as

$$\begin{aligned} \dot{x}_l &= (A_{ln} + \delta_v A_{lv})x_l + (B_{ln} + \delta_v B_{lv})w_l \\ &= (A_{ln} \ B_{ln}) \begin{pmatrix} x_l \\ w_l \end{pmatrix} + \delta_v (A_{lv} \ B_{lv}) \begin{pmatrix} x_l \\ w_l \end{pmatrix} = (A_{ln} \ B_{ln}) \begin{pmatrix} x_l \\ w_l \end{pmatrix} + w_v \end{aligned} \quad (10)$$

where

$$w_v = \delta_v (A_{lv} \ B_{lv}) \begin{pmatrix} x_l \\ w_l \end{pmatrix} = \delta_v z_v, \quad z_v = (A_{lv} \ B_{lv}) \begin{pmatrix} x_l \\ w_l \end{pmatrix}. \quad (11)$$

In (11), w_v and z_v represent the input and output signals of the disturbance channel corresponding to the time-varying parameter v_a . Rewrite equations (10), (11), and (2) in a matrix form as

$$\begin{pmatrix} \dot{x}_l \\ z_v \\ y_l \end{pmatrix} = \begin{pmatrix} A_{ln} & B_{lw} & B_{ln} \\ A_{lv} & B_{lz} & B_{lv} \\ C_{ln} & D_{lw} & D_{lu} \end{pmatrix} \begin{pmatrix} x_l \\ w_v \\ w_l \end{pmatrix}, \quad (12)$$

$$w_v = \Delta_v z_v, \quad \Delta_v = \delta_v I_4 \quad (13)$$

where $B_{lw} = I_4$ is an 4×4 unity matrix, $B_{lz} = Z_4$ is an 4×4 zero matrix, $D_{lw} = D_{lu} = 0$. Δ_v is also called the perturbation block. Let G_{la} be the transfer function with the state-space realization (12), i.e.

$$G_{la} \triangleq \left[\begin{array}{c|c} A_{ln} & B_{ln} \\ \hline C_{ln} & D_{lu} \end{array} \right] = \left[\begin{array}{c|cc} A_{ln} & B_{lw} & B_{ln} \\ \hline A_{lv} & B_{lz} & B_{lv} \\ C_{ln} & D_{lw} & D_{lu} \end{array} \right]. \quad (14)$$

The system can then be generally described by

$$\begin{pmatrix} z_v \\ y_l \end{pmatrix} = G_a \begin{pmatrix} w_v \\ w_l \end{pmatrix} = \begin{pmatrix} G_{zw} & G_{zu} \\ G_{yw} & G_{yu} \end{pmatrix} \begin{pmatrix} w_v \\ w_l \end{pmatrix}, \quad (15)$$

where G_{yu} is the transfer function mapping w_l to y_l .

3. H_∞ control design

In this section, we start with H_∞ -synthesis for the above mentioned frozen values of the aircraft forward speed. Then the performance of the linear time-invariant (LTI) controller designed for a fixed value of v_a is evaluated with other constant values of its. The content of this section is similarly to one in [8] but this design is for MIMO systems in stead of SISO ones.

3.1. H_∞ loop shaping design

A standard control structure for the synthesis of an H_∞ -controller is depicted in Figure 2. Here, Δ_v is the uncertainty block as given in (13), K_{le} is the H_∞ controller that is to be designed. In this configuration, the reference input is $r_l = (u_d \ \alpha_d)^T$, $(\delta_E \ \beta_T)^T$ is the controller output, $y_l = (u \ \alpha)^T$ is the controlled output, and $e_{le} = r_l - y_l$ is the controller input which is equal to the tracking error.

The interconnection of the system used for the controller synthesis is shown in Figure 3 where G_{ln} is the LTI part of the plant as given in (14). The external control input w_{le} consists of the throttle servo and the angle of attack $w_{le} = (u_d \ \alpha_d)^T$. The controlled variable is $z_{le} = (z_t \ z_s)^T$. Note that the component β_T of the external control inputs are considered as disturbances and their influences on the controlled outputs must be reduced as much as possible.

The weighting function W_s is used to shape the transfer function from the external control input w_{le} to the tracking error e_{le} . W_s is kept large over the low frequency range for tracking. The weighting function W_t is used to shape the transfer function from the external control input w_{le} to the controlled output y_r . The selection of the weighting

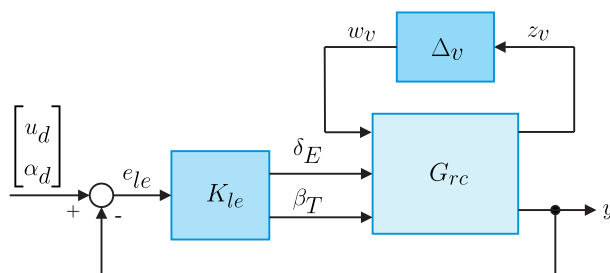


Figure 2. Structure of the closed-loop system in H_∞ design

function W_t is not only intended to keep the closed loop bandwidth at a desired value, but also to reject the effects of the component β_T on the controlled outputs as discussed above. Note that a large bandwidth corresponds to a faster rise time but the system is more sensitive to noise and to parameter variations [12].

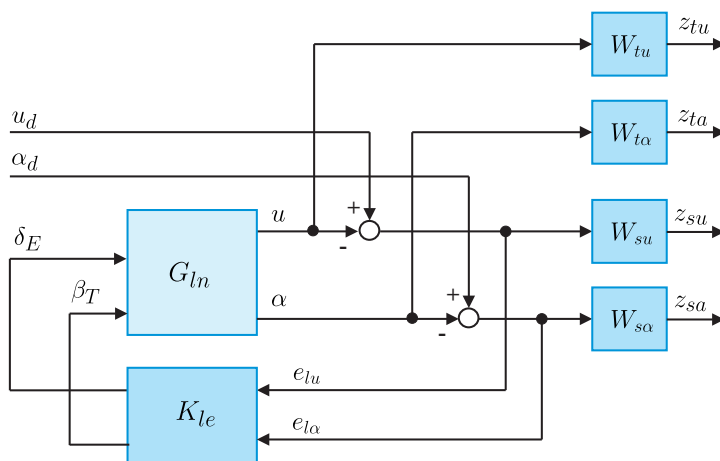


Figure 3. The interconnection of the system

The standard H_∞ control problem is to find a stabilizing LTI controller K_{le} at fixed frozen values of v_a such that the H_∞ -norm of the channel $w_{le} \rightarrow z_{le}$ is smaller than a given number γ :

$$\left\| \begin{pmatrix} W_s S_{le} \\ W_t T_{le} \end{pmatrix} \right\|_\infty \leq \gamma.$$

3.2. Simulation results with the H_∞ current controller

The set of the aircraft parameters that is given as follows [1]: $\theta_e = 0$, $\frac{Z_u}{m} = -0.36 / s$, $\frac{X_\alpha}{m} = 1.96 m/s^2$, $\frac{Z_\alpha}{m} = 108 m/s^2$, $\frac{M_\alpha}{J_{yy}} = -8.6 / s^2$, $\frac{M_{\dot{\alpha}}}{J_{yy}} = -0.9 / s$, $\frac{M_q}{J_{yy}} = -2 / s$, $\frac{X_\delta}{m} \approx 0$, $\frac{Z_\delta}{m} = 0.3 m/s^2/rad$, $\frac{M_\delta}{J_{yy}} = 0.1243 s^{-2}$, $\frac{X_T}{m} = 0.2452 m/s^2/rad$, $\frac{Z_T}{m} \approx 0$, and $\frac{M_T}{J_{yy}} \approx 0$. During the controller design stage, a trial-and-error-repetition technique is used in order to achieve the desired performance specifications by adjusting the weighting functions. The design steps were repeated until we are able to meet the required performance specifications. Finally, the following weighting functions were obtained:

$$W_t = (W_{tu} \ W_{ta})^T, \quad W_{tu} = \frac{0.5}{1.15s + 1.98}, \quad W_{ta} = \frac{0.5}{1.15s + 1.98}, \quad (16)$$

$$W_s = (W_{su} \ W_{sa})^T, \quad W_{su} = \frac{1}{5s + 1.05}, \quad W_{sa} = \frac{0.99}{5s + 1.05}. \quad (17)$$

For the chosen frozen value of $U = 55\text{m/s}$, the controlled system with the H_∞ current controller for the above given weighting functions achieves a norm of 0.943.

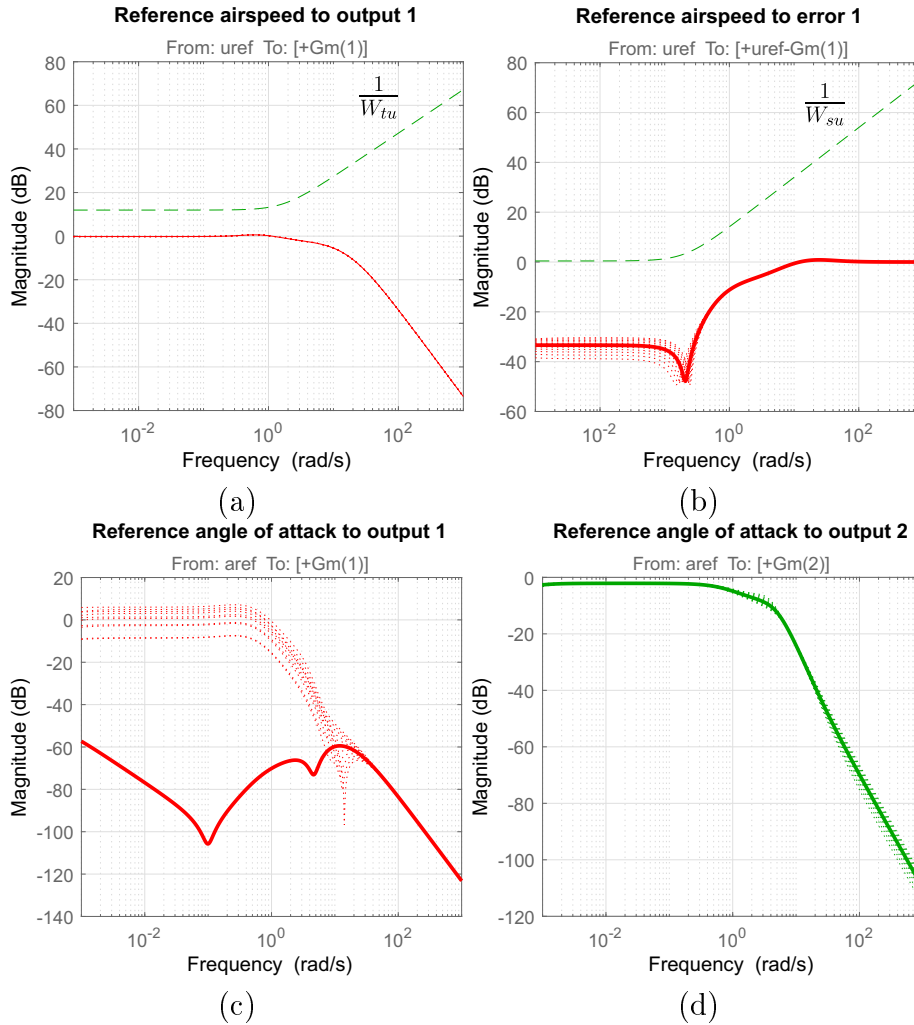


Figure 4. The performance of the controlled system with H_∞ current controller in the frequency domain for the variation of v_a from $0.5v_n$ to $1.5v_n$.

Figure 4 shows the frequency responses of the controlled system with the H_∞ current controller and the inverse of the weighting functions W_{tu} (see equations (16) and (17)) with 11 frozen values of the aircraft forward speed from 50% up to 150% of its nominal magnitude. In this figure, the thick solid lines show the responses of the closed-loop system with respect to the normal value of the aircraft speed. Figures 4a,b show the relevant magnitude plots of the complementary sensitivity and sensitivity functions of the closed-loop system with the performance requirements achieved by W_t and W_s . Figure 4a shows the response of the output u with respect to the reference inputs u_d .

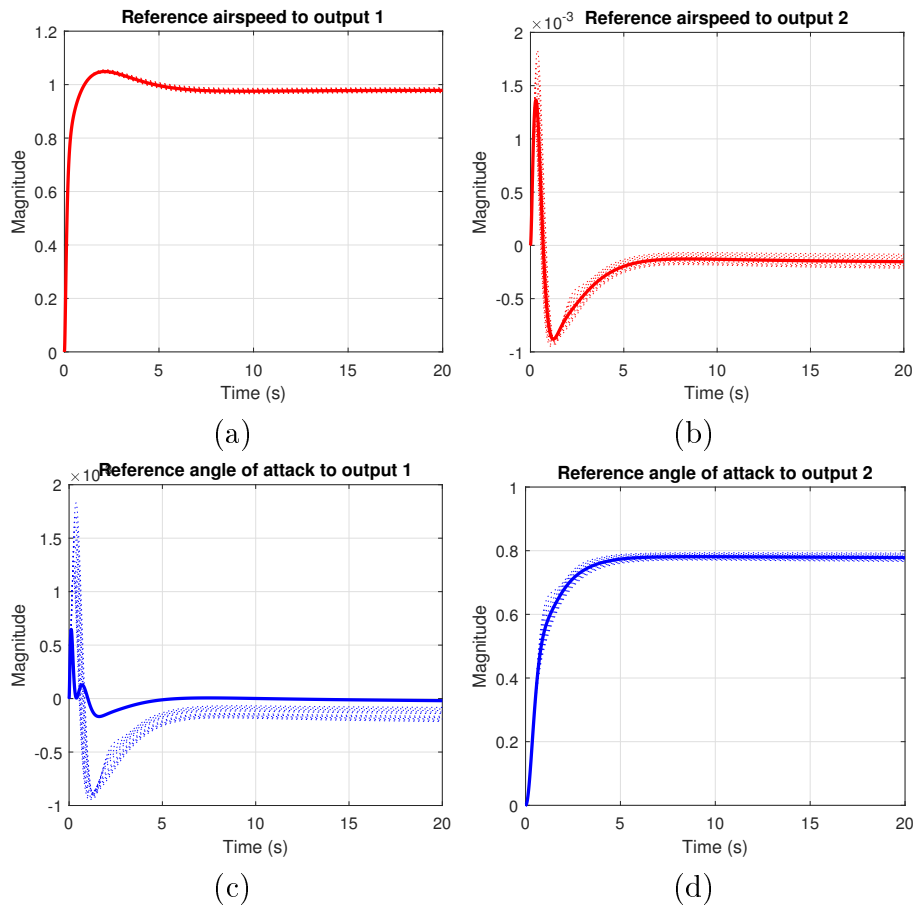


Figure 5. The performance of the controlled system with H_∞ current controller in the time domain for the variation of v_a from $0.5v_n$ to $1.5v_n$.

The performance of the reference input u_d to the control error $u_d - u$ is shown in Figures 4b. The inverse of the weighting function W_{tu} (see Figure 3) is depicted by the dashed line in Figure 4a and the inverse of the weighting function W_s is depicted by the dashed lines in Figure 4b, respectively. Figures 4c,d show the relevant magnitude plots of the transfer functions from the reference input α_d to output u and α , respectively.

It is clear from Figure 4 that the sensitivity and complementary sensitivity functions are below the inverse of the performance weighting functions. The gains of the frequency responses of the reference angle of attack for some values of aircraft speeds are bigger than zero. This indicates that the influence of crossing-terms into the channel from reference airspeed to its output is not small. Note that these performance curves are obtained for 11 values of the aircraft forward speeds as mentioned above.

Figure 5 shows the time responses of the controlled system for a step input in the consistence to the curves in the frequency domain as shown in Figure 4 with 11 values of the aircraft forward speed as shown above.

4. Conclusion

This paper has briefly presented an LMI-based loop-shaping design of the multiple-input multiple-output robust H_∞ controller for the linear simplified longitudinal model of a aircraft, in which the aircraft forward speed is considered as an uncertain param-

eter. The robust H_∞ controller is then synthesized to guarantee that the H_∞ -norm of the closed-loop system is smaller than some given number for different frozen values of the aircraft forward speed. Next, the robust performance of the robust controller with respect to the other the aircraft forward speeds is investigated in the range from 50% up to 150% of its nominal values. Some simulation results are given to demonstrate the performance and robustness of the control algorithm. Since the effect of the crossing-term in the aircraft model was not small, it is difficult to obtain good tracking performance for both channels from the reference airspeed to its output as well as from the reference angle of attack to its output. Therefore, this problem should be take into account for improving the tracking performance of the closed-loop control system in future works.

REFERENCES

- [1] A. Tewari, *Advanced control of aircraft, spacecraft and rockets*. Wiley, 2011.
- [2] J. Zarei, A. Montazeri, M. R. J. Motlagh, and J. Poshtan, "Design and comparison of LQG/LTR and H_∞ controllers for a VSTOL flight control system," *Journal of the Franklin Institute*, vol. 344, no. 5, pp. 577–594, 2007.
- [3] B. Lu, F. Wu, and S. W. Kim, "Switching LPV control of an F-16 aircraft via controller state reset," *IEEE Transactions on Control Systems Technology*, vol. 14, no. 2, pp. 267–277, 2006.
- [4] R. A. Hyde, "The application of robust control to VSTOL aircraft," Ph.D. dissertation, Girton College Cambridge, 1991.
- [5] N. Aouf and B. Boulet, "Linear fractional transformation gain-scheduling flight control preserving robust performance," *Journal of Aerospace Engineering*, vol. 226, no. 7, pp. 763–773, 2011.
- [6] N. Wen, Z. Liu, Y. Sun, and L. Zhu, "Design of LPV-based sliding mode controller with finite time convergence for a Morphing aircraft," *International Journal of Aerospace Engineering*, vol. 11, pp. 955–969, 2017.
- [7] C. Weiser, D. Ossmann, and G. Looye, "Design and flight test of a linear parameter varying flight controller," *CEAS Aeronautical Journal*, vol. 11, pp. 955–969, 2020.
- [8] N. T. Hung and N. T. M. Huong, "A robust controller design for aircraft," *The conference of applying high technology into practice, Thainguyen University of Technology*, 2021.
- [9] N. T. Hung and N. D. Minh, "Performance of robust controller for DFIM when the rotor angular speed is treated as a time-varying parameter," *Vietnam Conference on Control and Automation, Hanoi*, 2011.
- [10] H. N. Tien, C. W. Scherer, J. M. A. Scherpen, and V. Muller, "Linear parameter varying control of doubly fed induction machines," *IEEE Transactions on Industrial Electronics*, vol. 63, no. 1, pp. 216–224, 2016.
- [11] N. T. M. Huong and N. T. Hung, "Robustness stability analysis for H-infinity control of separately excited DC motors," *TNU Journal of Science and Technology*, vol. 188, pp. 29–37, 2018.
- [12] S. Skogestad and I. Postlethwaite, *Multivariable feedback control - Analysis and design*. John Wiley & Sons, 1996.